

Local order and magnetic field effects on the electronic properties of disordered binary alloys in the Quantum Site Percolation limit

D. F. de Mello

*Departamento de Física, Faculdade de Ciências,
Universidade Estadual Paulista (UNESP),
C. P. 473, Bauru 17033-360, SP, Brazil*

G. G. Cabrera

*Instituto de Física “Gleb Wataghin,”
Universidade Estadual de Campinas (UNICAMP),
C. P. 6165, Campinas 13083-970, SP, Brazil*

(Received)

Abstract

Electronic properties of disordered binary alloys are studied *via* the calculation of the average Density of States (DOS) in two and three dimensions. We propose a new approximate scheme that allows for the inclusion of local order effects in finite geometries and extrapolates the behavior of infinite systems following *finite-size scaling* ideas. We particularly investigate the limit of the Quantum Site Percolation regime described by a tight-binding Hamiltonian. This limit was chosen to probe the role of short range order (SRO) properties under extreme conditions. The method is numerically highly efficient and asymptotically exact in important limits, predicting the correct DOS structure as a function of the SRO parameters. Magnetic field effects can also be included in our model to study the interplay of local order and the shifted quantum interference driven by the field. The average DOS is highly sensitive to changes in the SRO properties, and striking effects are observed when a magnetic field is applied near the *segregated* regime. The new effects observed are twofold: there is a reduction of the band width and the formation of a gap in the middle of the band, both as a consequence of destructive interference of electronic paths and the loss of coherence for particular values of the magnetic field. The above phenomena are periodic in the magnetic flux. For other limits that imply strong localization, the magnetic field produces minor changes in the structure of the average DOS.

I. INTRODUCTION

Considerable efforts have been made in the understanding of localization properties of electronic states of disordered systems since the work by Anderson.¹ Being the simplest one to investigate the above phenomena, the Anderson model is formulated through a Tight Binding Hamiltonian with diagonal disorder and hopping t to nearest neighbors. The site energies are randomly distributed within some range W , and W/t is the relevant parameter to distinguish between the strong and weak localization regimes. Anderson showed that disorder, in three dimensional systems, drives a metal-insulator transition, with a mobility edge separating localized from extended electronic states.

The one parameter scaling theory, introduced by Abrahams *et al.*,² predicts that all states are localized for dimensions smaller than or equal to two. Dimension two then appears as a marginal case. The one-parameter scaling hypothesis assumes that the conductance of a finite sample scales in a universal way, and has been supported by several experiments done in the early 1980s,³ and by a large number of numerical works.⁴⁻⁶ However, it has been suggested that the theory breaks down when electron-electron interactions are included, or when an external magnetic field is applied.^{7,8} Remarkable new experiments on 2D electron systems,⁹ in samples with much higher electron mobilities than the previous ones, do show a clear evidence for a metal-insulator transition at low electron densities, in the absence of a magnetic field. The effect has been ascribed to the dominant role of Coulomb interactions, and a new scaling theory has been proposed for interacting electrons,¹⁰ leaving open the possibility of a 2D metal.

Within the one-electron scheme, it was well known that in 2D, the effect of back scattering from impurities is enhanced, leading to an insulating behavior at zero temperature. Electron trajectories interfere constructively in the backward direction, and one gets localization for any degree of disorder. Transport properties with an external magnetic field are useful probes to test the above effects. Quantum interference of electron trajectories, modified by the applied field, may change the localization properties of the electron wave function. One evidence of this fact is the observation of magnetoresistance oscillations with an applied field in thin disordered metallic cylinders.^{11,12} With this geometry, and orienting the field along the cylinder axis, one can select the phase of the electron orbits in order to observe the phenomenon macroscopically. For two-dimensional systems, like the ones realized in semiconductor heterostructures, it has been observed a metal-insulator transition induced by the magnetic field.¹³ Samples that, at sufficiently low temperatures and zero field, exhibits a localized electronic behavior, present evidence of extended states at strong magnetic fields. Other evidences for a transition to a metallic regime have been observed in experimental studies of the magnetoresistance and magnetoconductance.^{14,15} As a general rule, quantum interference effects are invoked to explain the delocalization of the electronic wave function with the field.⁸ The reentrant behavior of the magnetoresistance found by some authors at very high magnetic fields,^{16,17} is associated with the shrinkage of the electronic wave function.¹⁸

One effect marginally taken into account, and that may have important consequences, even within the one-electron picture, is the inclusion of Short-Range Order (SRO) correlations in the electronic properties of disordered systems.^{19,20} Real disordered systems are not necessarily random, but may present different degrees of short-range order. In a binary alloy,

for given concentrations of the atomic species, one may get configurations ranging from segregation to complete order as a function of the SRO properties. In this work we investigate the role of the above effects and its interplay with the action of an applied magnetic field, in The Quantum Site Percolation limit. The latter regime corresponds to the case where the two site energies, for a binary alloy, are very far apart in the energy scale, and *percolation* of the wave function is only possible through atoms of the same species. Thus, this limit favors localization when short range correlates atoms of different kind as nearest neighbors. We remark that this case is difficult to calculate within other approximations of nonlocal character.²⁰ We calculate the average electronic Density of States (DOS) using a previously developed method reported in Ref. 19. Our approach relies on one dimensional numerical techniques, and is efficiently applied to long stripes and bars of finite cross section with the idea that two and three dimensional lattices may be obtained by joining infinite linear chains. From grounds based on Statistical Mechanics results,²¹ this geometry, generically called as *cylindric*, is expected to converge more rapidly to the bulk limit than the simpler block geometry. Indeed, for the disordered case, the bulk regime can be extrapolated with a relatively small number of chains. SRO effects are included following the Kikuchi method,²² where correlations are systematically handled. The last step in the calculation involves a configurational average, where the probability of a given configuration is obtained in terms of the short and long range order parameters. The electronic DOS calculated through the above procedure, in spite of being an average, is rich in structures, and as we will show below, is highly susceptible to changes in local properties.

Magnetic field effects are considered with the introduction of a phase in the electronic hopping term⁸ *via* the so called Peierls substitution.²³ This phase is related to the magnetic flux across an elementary cell, as given by the well known Aharonov-Bohm effect.²⁴ The lattice model approach adopted in this paper is known to accurately describe the lowest Landau level in the situation where the disorder broadening is such that no overlap of magnetic sub-bands occurs. We are also neglecting electron-electron interactions and electron spin (spin-split Landau levels), and all the effects found in the present contribution are exclusively due to disorder in a one-particle lattice model. We found that magnetic field effects are stronger near the segregation limit, where one expects weak localization properties and a higher degree of coherence in the electronic wave function. An oscillatory behavior of the electronic DOS is observed as a function of the field, with surprising effects on the structure of the DOS.

Our paper is organized as follows: In the next Section we present the method to calculate the DOS. As illustrative examples, we show results for one-component non-disordered samples in two and three dimensions. The two-dimensional disordered case including SRO effects is also shown for completeness. In Section III we extend our calculation to three-dimensional disordered systems in the presence of an applied magnetic field. Finally, in Section IV we present and discuss numerical results for several examples of the latter.

II. A NEW APPROACH TO CALCULATE THE DOS

The computational scheme that will be employed here, was developed previously by the authors to study the electronic DOS in two-dimensional disordered binary alloys.¹⁹ For completeness, we discuss in this Section some details of the method and present the extension

to three dimensions in the next Section.

A tight-binding Hamiltonian for a single s -atomic-like orbital, in a hypercubic lattice structure in d dimensions, yields the following dispersion relation in k -space:

$$E(\mathbf{k}) = E_0 + \sum_{i=1}^d 2V \cos k_i a, \quad (1)$$

where E_0 is the atomic energy, V is the hopping (kinetic) term for nearest neighbors in a pure system, and a is the lattice parameter. The DOS for d -dimensional systems can be obtained recursively from the DOS in $(d-1)$ dimensions, in the form of a convolution with the DOS of a linear chain

$$\mathcal{D}^{(d)}(E) = \int dE' \mathcal{D}^{(d-1)}(E') \mathcal{D}^{(1)}(E - E'). \quad (2)$$

This result is shown analytically in the Appendix for two dimensions. For a finite system with the geometry of a *hyper-cylinder*, like a strip with finite width, the DOS is obtained as a discrete convolution of the DOS of the linear chain with the distribution of eigenvalues for the finite transverse section of the cylinder

$$\mathcal{D}_{Cylinder}^{(d)}(E) = \sum_i \mathcal{D}_{Section}^{(d-1)}(E_i) \mathcal{D}^{(1)}(E - E_i) \quad (3)$$

In finite systems, strong oscillations are present in the DOS, specially near the points where van Hove singularities are developed in the infinite limit (in analogy with the so called Gibbs phenomenon for Fourier series). The above oscillations are typical size effects, with the amplitude being damped when the size of the finite section is increased.²⁵ In Fig.1 we display the DOS for the square lattice for wide but finite width stripes, along with the infinite two dimensional case (uppermost figure). The corresponding three dimensional case (cubic lattice) is depicted in Fig.2. We compare finite bar geometries with the infinite three dimensional limit. The energy scale is given in units of V , the hopping integral. The large amplitude of oscillations are due to coherence effects in pure samples, and as we will show later, size effects decay more rapidly in disordered systems. In addition, as remarked in the Introduction, the *cylindric* geometry, with an infinite dimension along the axis, is expected to converge considerably faster to the bulk limit than the block geometry. This latter fact allows the use of relatively small samples to extrapolate the DOS of disordered alloys. One comment is in order here. As shown in expression (3), the DOS for a finite system is obtained as a weighted superposition of one-dimensional densities. The interchain coupling displaces the center of gravity of the one-dimensional DOS to the *renormalized* value E_i , which takes into account the true coordination number and the degrees of freedom of the transverse section of the system. The weight in (3) for each chain is exactly the discrete density of the eigenvalues $\{E_i\}$.

The above exact analytic results are extended heuristically to treat disordered systems. In this Section we show the procedure for two dimensions,¹⁹ where the transverse part of the system is a finite chain. Local order effects are handled with a single variable, the so called Cowley's parameter σ ²⁶:

$$\sigma = 1 - \frac{p_{AB}}{c_{AC}c_B}, \quad (4)$$

with p_{AB} being the probability of having an AB pair, and c_A and c_B the concentrations for species A and B respectively. With the above definition, σ ranges from -1 (limit of complete local order) to 1 (limit of segregation), passing through intermediate cases with variable local order that include the random limit for $\sigma = 0$. For Markovian chains, SRO effects were embodied in a numerically exact algorithm based on the so called Negative Factor Counting (NFC) method²⁷ to calculate the DOS for such systems. Our scheme thus relies on exact calculations for $\mathcal{D}^{(1)}(E; \sigma)$, the DOS of disordered infinite chains with local order described by σ . To get the analogous of expression (3) for a disordered two-dimensional stripe of width M , we generate all the configurations of a finite chain of M sites, and get the corresponding eigenvalues and their multiplicities. For a given configuration, the DOS is obtained as

$$\mathcal{D}_{Strip}^{(2)}(E; M, c) = \sum_{i=1}^M d_{Section}^{(1)}(E_i; M, c) \mathcal{D}^{(1)}(E - E_i; \sigma), \quad (5)$$

where the $\mathcal{D}^{(1)}(E - E_i; \sigma)$ is an infinite chain DOS with the center of gravity displaced to E_i , the eigenvalues of the finite transverse chain for the given configuration. Each term of the sum (5) is weighted by $d_{Section}^{(1)}(E_i; M, c)$, the discrete distribution of the eigenvalues $\{E_i\}$. The final DOS is an average over all the possible configurations:

$$\mathcal{D}_{strip}^{(2)}(E) = \sum_c P_c \mathcal{D}_{Strip}^{(2)}(E; M, c), \quad (6)$$

with P_c equal to the probability of a given configuration c . The latter is obtained, for Markov chains,²⁸ as a weighted product of pair probabilities and depends only on σ and the concentrations. In Fig.3 we show the lowest sub-band for 50-50% alloying with different degrees of SRO in two dimensional strips of width $M = 20$. In spite of the finite size, the three cases already display two dimensional features characteristic of the infinite limit. The DOS structure changes dramatically as a function of the local order, with highly localized states near the random and ordered limits. The upper figure is close to the segregation limit and resembles the pure case shown in Fig.1. For this regime, the electronic wave function may percolate through atoms of the same type in very large islands. In contrast with one dimension, the above properties are typical of the two dimensional topology, with many different percolation paths for extended electron trajectories.

For three dimensions, the finite section is of two dimensional character and SRO properties are handled with more parameters that include the possibility of closed path correlations. This is done using the Kikuchi method²² and is described in the next Section.

III. THE INCLUSION OF MAGNETIC FIELDS AND SRO PROPERTIES IN THREE-DIMENSIONAL GEOMETRIES

Following ideas developed in Finite-Size Scaling methods,⁴ our system is taken as a bar in three dimensions, with finite dimensions in the x and y directions, and infinite extension along the z direction. Periodic boundary conditions are imposed for the finite section of the system. The magnetic field is applied parallel to the z axis.

We model our system using an Alloy Tight Binding (ATB) Hamiltonian:

$$\mathcal{H} = \sum_{\langle i \rangle} E_i |i\rangle \langle i| + \sum_{\langle ij \rangle} V e^{i\phi_{ij}} |i\rangle \langle j| + h.c., \quad (7)$$

where off-diagonal elements are taken different from zero only for nearest neighbors, and ϕ_{ij} is a phase that represents the effect of the magnetic field in an elementary cell with the lattice parameter as a side (Peierls substitution²³). For simplicity, we choose the hopping amplitude as real along the x axis ($\phi = 0$), and complex along the y axis. The phase difference between two successive bonds is related to the magnetic flux enclosed in an elementary cell,

$$\phi_{n+1} - \phi_n = \frac{e}{\hbar c} \oint \vec{A} \cdot \vec{ds} \quad , \quad (8)$$

where \vec{A} is the associated electromagnetic vector potential. Periodic boundary conditions for the finite section of the system induce a quantization of the magnetic flux that depends on the size of the sample. One can get rid of the above constraint by choosing free ends, but in this case finite size effects decay more slowly.

As mentioned in the previous Section, we studied the limit corresponding to the Quantum Site Percolation case, where $|E_A - E_B| \gg V$. SRO is treated using the Kikuchi method with closed square diagrams as highest order correlations.²² This approximation is known to correctly describe the two dimensional topology. For each square we have 16 different configurations. These configurations are displayed in Fig.4, with the respective probabilities (z'_i s) and degeneracies (β'_i s).

Normalization conditions require:

$$c_A + c_B = 1 \quad (9)$$

for concentrations,

$$\begin{aligned} p_{AA} + p_{AB} &= c_A \\ p_{BB} + p_{AB} &= c_B \end{aligned} \quad (10)$$

for pairs, and

$$\begin{aligned} p_{AA} &= z_1 + 2z_2 + z_3 \\ p_{AB} &= z_2 + z_3 + z_4 + z_5 \\ p_{BB} &= z_3 + 2z_5 + z_6 \end{aligned} \quad (11)$$

for squares.

In all, we get 5 independent parameters, which are chosen to be p_{AB} , z_3 , z_4 , ξ_1 and ξ_2 , with the last two defined as:

$$\begin{aligned} \xi_1 &= c_A - c_B \\ \xi_2 &= z_2 - z_5. \end{aligned} \quad (12)$$

While the first three parameters (p_{AB}, z_3, z_4) are related to correlations of short range, the last two (12) handle long range order.

Dependent variables are written as:

$$\begin{aligned}
c_A &= (1 + \xi_1)/2 \\
c_B &= (1 - \xi_1)/2 \\
p_{AA} &= (1 + \xi_1 - 2p_{AB})/2 \\
p_{BB} &= (1 - \xi_1 - 2p_{AB})/2 \\
z_1 &= (1 + \xi_1 - 4p_{AB} + 2z_4 - 2\xi_2)/2 \\
z_2 &= (p_{AB} - z_3 - z_4 + \xi_2)/2 \\
z_5 &= (p_{AB} - z_3 - z_4 - \xi_2)/2 \\
z_6 &= (1 - \xi_1 - 4p_{AB} + 2z_4 + 2\xi_2)/2
\end{aligned} \tag{13}$$

Within the approximation adopted, a given configuration of the finite section is obtained by joining squares. The corresponding probability is obtained as a product of conditional square probabilities, where the constraint is that two squares are linked by a common bond. This approach has been devised in analogy to Markovian chains,²⁸ but with the square as the basic correlation.

As it will be seen in the next Section, our method allows to include local properties under the coupled effects of variable disorder and application of a magnetic field.

IV. NUMERICAL RESULTS AND DISCUSSION

In the examples that follow, we consider 50-50% alloying and several degrees of local order. The site energies are taken to be $E_A = 0$ and $E_B = 1000$, in units of the hopping term V . In all the figures, we only display the lowest sub-band, the one centered at E_A . Fig.5 shows examples calculated in the absence of a magnetic field: (a) near the ordered limit; (b) random disorder; and (c) near the limit of segregation. The behavior is similar to the one shown previously for two dimensions. Near the segregated limit the DOS for each sub-band resembles the one of the pure case, suggesting the presence of extended electronic states. On the other hand, when the system is near the ordered limit, the DOS shows the typical structure of localized states, as it should be expected for two kinds of atoms with very different site energies. In this instance, the probability for one state to propagate is nearly zero, due to almost infinite barriers. The authors are currently calculating other cases where the centroids approach to each other, and the bands overlap. In this situation, quantum diffusion is possible by means of tunneling through high but finite barriers, and a delocalization onset is expected as a function of the band separation.²⁹ To illustrate the role of local order, in Fig.6 we display the DOS values for three nearby energy levels as a function of the correlation σ , in two dimensions. One of the levels corresponds to a sharp peak in the middle of the band in the lowest part of Fig.3, for $\sigma = 0$.

Size effects are pictured in Fig.7 for the random alloy. It is worth noting that the DOS of finite systems already present the whole structure of the infinite case, even for small transverse sections. This seems to be characteristic of the bar geometry, where one of the dimensions is infinite and the bulk limit is extrapolated with not too big cross sections. Due to numerical limitations, the next examples in the presence of a magnetic field, are calculated in finite geometries only (sections of 12 atoms).

We now analyze the role of the magnetic field. In Fig.8 we show the DOS for a case near the segregation limit. An oscillatory behavior of the DOS with the field is observed,

and the figure depicts cases up to half the period in the flux. The values are adjusted to periodic boundary conditions. The effect is paramount at the center of the sub-band, with the appearance of a gap for $\Delta\phi = \pi$. The phenomenon is due to destructive interference of the electronic paths in the presence of the field. The band width is also affected, with a striking reduction at half a period.

On the other hand, tiny effects are observed near the random and ordered limits, with no sensitive changes in the structure of the DOS as a function of the field. Other cases with different concentrations were also calculated. As a general rule, the DOS structure is more affected by the field near the so called *weak localization* regime, when the concentration of one of the species is small. Localization and delocalization of electronic states may be interpreted as pure quantum effects due to destructive or constructive interference of the different electronic paths. This interference is shifted by the application of a field. In Fig.9, we show the effect of the magnetic field on a particular level as a function of short-range correlations. The figure displays a trajectory in our parameter space, ranging from the local ordered limit to the segregated case. This trajectory, for short, is labeled with the symbol σ . The figure pictures in a different way our comments above: the DOS oscillates as a function of the field, but the effect predominates in the vicinity of the segregated limit (for $0.5 \leq \sigma \leq 1$ in the figure).

In summary, it has been shown that the method proposed is numerically efficient, reproduces the DOS in important limits, and predicts new behaviors as function of the SRO and magnetic field. To theoretically investigate localization properties, one needs to calculate the electron wave function, or get indirect information *via* the so called localization length. In two and three dimensions, most of the works in the literature concentrate around simulations or other numerical techniques. As a common characteristic, they are based on Finite Size Scaling methods, but most of the cases investigated correspond to random disordered systems, represented generally by the Anderson Model or the Quantum Percolation Model^{5,6}. Our results, in spite that we calculate the average *DOS*, suggest that *SRO effects may play an important role in the localization of electronic states*. A phase diagram in which the degree of localization is displayed, may depend not only on the concentrations, but also on the SRO parameters. In order to illustrate this issue, we suggest numerical computations of the localization length in systems like the ones considered here, with equal concentrations of the species, very different site energies, and variable local order properties. Changes in the localization properties will then be entirely ascribed to short-range correlations.

The applied magnetic field strongly changes the electronic properties in the *weak localization* limit. On the other hand, in the opposite regime, the effects of the field on the average DOS are negligible. Huge magnetic fields are involved in the above phenomena due to the small size of the elementary cell. However, the effects predicted here may be brought to a range susceptible of observation in the case of superlattice structures, or in geometries where the electronic paths enclose macroscopic areas that contribute to the flux. We note that the present state of the art in nanostructure technology allows the fabrication of modulated 2D systems with lattice parameters of the order of 100 nm or more (see for instance Ref. 30).

ACKNOWLEDGMENTS

The authors are grateful to Professors D. Gottlieb, B. Laks, N. Majlis, and P. Schulz for helpful discussions. This work was partially financed by a grant from *Vitae* (Brazil, Project No. B-11487/2B9221). One of the authors (G.G.C.) also acknowledges support from *Conselho de Desenvolvimento Científico e Tecnológico* (CNPq, Brazil, Project No.301221/77-4).

APPENDIX A: EXACT CALCULATION FOR THE DOS IN TWO DIMENSIONS

The DOS for the pure cubic lattice in d dimensions was given in Section II by eq.(2). We show explicitly this result for the two-dimensional case.

If we consider that states $\{|m, n\rangle\}$ represent the basis in the site representation, where the indexes are integers along the x and y axes respectively, the Hamiltonian reads:

$$\begin{aligned} \mathcal{H} = \sum_{\langle m, n \rangle} E_{mn} |m, n\rangle \langle m, n| + \sum_{\langle n \rangle} t_x |m, n\rangle \langle m, n+1| + h.c. \\ + \sum_{\langle m \rangle} t_y |m, n\rangle \langle m+1, n| + h.c. \end{aligned} \quad (\text{A1})$$

Taking the Fourier transform in relation to the x direction:

$$|m, n\rangle = \frac{1}{\sqrt{N}} \sum_{\langle k_0 \rangle} e^{ikn} |m, k\rangle \quad , \quad (\text{A2})$$

we get:

$$\begin{aligned} \mathcal{H} = \sum_{m, k} (E_0 + 2t_x \cos k) |m, k\rangle \langle m, k| + \\ \sum_{m, k} t_y (|m, k\rangle \langle m+1, k| + |m+1, k\rangle \langle m, k|) . \end{aligned} \quad (\text{A3})$$

The Green's function in the basis $\{|m, k\rangle\}$ is given by:³¹

$$\mathbf{G}(z) = \sum_{m, k} \frac{|m, k\rangle \langle m, k|}{z - E(k, m)}, \quad (\text{A4})$$

where $E(k, m)$ are the eigenvalues:

$$E(k, m) = E_0 + 2t_x \cos k + \lambda_m = E_x(k) + \lambda_m, \quad (\text{A5})$$

with:

$$E_x(k) = E_0 + 2t_x \cos k, \quad (\text{A6})$$

and λ_m corresponding to the eigenvalue of an *effective* chain with site energy $E_0 + 2t_x \cos k$ and hopping t_y between first neighbors along the y direction.

The Green's function can be rewritten as:

$$\mathbf{G}(z) = \sum_{m,k} \frac{|m, k\rangle \langle m, k|}{z - E_x(k) - \lambda_m}, \quad (\text{A7})$$

with the diagonal element:

$$\langle m, n | \mathbf{G}(z) | m, n \rangle = \frac{L}{2\pi N} \int_{BZ} dk \frac{1}{z - \lambda_m - E_x(k)} \quad (\text{A8})$$

The DOS and the Green's function satisfy the relation³¹:

$$\mathcal{D}(E) = -\frac{1}{\pi} \text{Im} \sum_{m,n} \langle m, n | \mathbf{G}(E) | m, n \rangle, \quad (\text{A9})$$

with:

$$\frac{1}{NM} \sum_{m,n} \langle m, n | \mathbf{G}(z) | m, n \rangle = \frac{1}{M} \sum_m \frac{1}{2\pi} \int_{-\pi}^{\pi} dk \frac{1}{z - \lambda_m - E_0 - 2t_x \cos(k)}, \quad (\text{A10})$$

and subsequently the DOS is given by:

$$\mathcal{D}(E) = \frac{1}{M} \sum_{\lambda_m} n(\lambda_m) \mathcal{D}_{1dim}(E - \lambda_m). \quad (\text{A11})$$

where $\mathcal{D}_{1dim}(E - \lambda_m)$ is the DOS of an infinite linear chain centered at λ_m , and $n(\lambda_m)$ is the degeneracy of the eigenvalue.

REFERENCES

- ¹ P. W. Anderson, Phys. Rev. **109**, 1492 (1958).
- ² E. Abrahams, P. W. Anderson, D. C. Licciardello and T. V. Ramakrishnan, Phys. Rev. Lett. **42**, 673 (1979).
- ³ P. A. Lee and T. V. Ramakrishnan, Phys. Rev. B **26**, 4009 (1982).
- ⁴ J. P. G. Taylor and A. Mackinnon, J. Phys.: Condens. Matter **1**, 9963 (1989).
- ⁵ A. Mackinnon and B. Kramer, Z. Phys. B **53**, 1 (1983).
- ⁶ C. M. Soukoulis and G. S. Grest, Phys. Rev. B **44**, 4685 (1991).
- ⁷ G. Bergman, Phys. Rep. **107**, 1 (1984).
- ⁸ B. Kramer and A. Mackinnon, Rep. Prog. Phys. **56**, 12 (1993).
- ⁹ S. V. Kravchenko *et al.*, Phys. Rev. B **51**, 7038 (1995).
- ¹⁰ V. Dobrosavljević *et al.*, Phys. Rev. Lett. **79**, 455 (1997).
- ¹¹ D. Yu Sharvin and Yu V. Sharvin, JETP Lett. **34**, 272 (1981).
- ¹² B. L. Altshuler, A. G. Aronov and B. Z. Spivak, JETP Lett. **33**, 94 (1981).
- ¹³ T. Wang, K. P. Clark, G. F. Spencer, A. M. Mack, and W. P. Kirk, Phys. Rev. Lett. **72**, 709 (1994).
- ¹⁴ Shih-Ying Hsu and J. M. Valles Jr., Phys. Rev. Lett. **74**, 2331 (1995).
- ¹⁵ S. Katsumoto, in *Localization 1990*, edited by K. A. Benedict and J. T. Chalker, Institute of Physics Conference Series Number 108 (Techno House, Bristol, 1991), p. 17.
- ¹⁶ J. P. Spriet, G. Biskupski, and H. Dubois, Phyl. Mag. B **54**, L95 (1986).
- ¹⁷ H. W. Jiang, C. E. Johnson, and K. L. Wang, Phys. Rev B **46**, 12830 (1992).
- ¹⁸ B. I. Shklovskii and A. L. Efros, *Electronic Properties of Doped Semiconductors* (Springer-Verlag, Berlin, 1984).
- ¹⁹ D. F. de Mello and G. G. Cabrera, Solid State Commun. **94**, 703 (1995).
- ²⁰ S. Weinketz, B. Laks, and G. G. Cabrera. Phys. Rev. B **43**, 6474 (1991).
- ²¹ G. G. Cabrera, R. Jullien, E. Brézin and J. Zinn-Justin, J. Physique **47**, 1305 (1986).
- ²² R. Kikuchi e Stephen G. Brush, J. Chem. Phys. **47**, 195 (1967).
- ²³ R. Peierls, Z. Phys. **80**, 763 (1933).
- ²⁴ J. J. Sakurai, *Modern Quantum Mechanics* (Addison-Wesley, Massachusetts, 1994), revised Edition.
- ²⁵ D. F. de Mello, R. E. Lagos, and G. G. Cabrera, to be published.
- ²⁶ M. Ziman, *Models of Disorder: The theoretical physics of homogeneously disordered systems* (Cambridge University Press, Cambridge, 1979).
- ²⁷ P. Dean, Rev. Mod. Phys. **44**, 127 (1972).
- ²⁸ J. Hubbard, Phys. Rev. B **19**, 1828 (1979).
- ²⁹ D. F. de Mello and G. G. Cabrera, to be published.
- ³⁰ T. Schlösser, K. Ensslin, J. P. Kotthaus, and M. Holland, Semicond. Sci. Technol. **11**, 1582 (1996).
- ³¹ E. N. Economou, *Green's Functions in Quantum Physics* (Springer-Verlag, Berlin, 1979), 2nd Edition.

FIGURES

FIG. 1. DOS, in arbitrary units, for a pure two-dimensional system: (a) upper figure, the exact two dimensional infinite sample; (b) middle, a strip with the finite transverse length $M = 500$; (c) lower, a strip with the finite transverse length $M = 100$. In all the cases, we take $E_A = E_B = 0$ and $V_{ij} = 1$, with energy steps equal to 5.10^{-4} .

FIG. 2. DOS, in arbitrary units, for the pure three-dimensional system: (a) upper figure, the exact three dimensional case obtained as the convolution of a two-dimensional DOS with a one-dimensional one; (b) middle, bar with $N \times M = 48$; (c) lower, a bar with $N \times M = 24$. For all the examples, $E_A = E_B = 0$ and $V_{ij} = 1$, with energy steps equal to 5.10^{-4} .

FIG. 3. DOS, in arbitrary units, for the square lattice with several degrees of SRO. All the cases shown in the figure were calculated for infinite stripes of width $M = 20$ chains. Concentrations are equal for both species and the Cowley parameter is given in each figure. Other parameters are $E_A = 0$, $E_B = 1000$, $V = 1$, with energy steps equal to 5.10^{-2} . We only display the lower sub-band: (a) upper figure, $\sigma = 0.8$, tendency to segregation; (b) middle, $\sigma = 0$, random alloy; (c) lower, $\sigma = -0.8$, tendency to ordering.

FIG. 4. Possible square configurations for two kinds of atoms (filled and empty circles). We denote by z_i 's the probabilities of each configuration, and the numbers indicated in the last column are the respective degeneracies.

FIG. 5. DOS, in arbitrary units, for the three-dimensional disordered case with several degrees of SRO. All the examples correspond to the infinite system, and were obtained by the convolution technique explained in the text. The concentrations of both species are equal, and as in previous examples, we use $E_A = 0$, $E_B = 1000$, $V = 1$, with energy steps equal to 5.10^{-2} . We only display the lower sub-band for the cases: (a) tendency to order; (b) random alloy; (c) tendency to segregation.

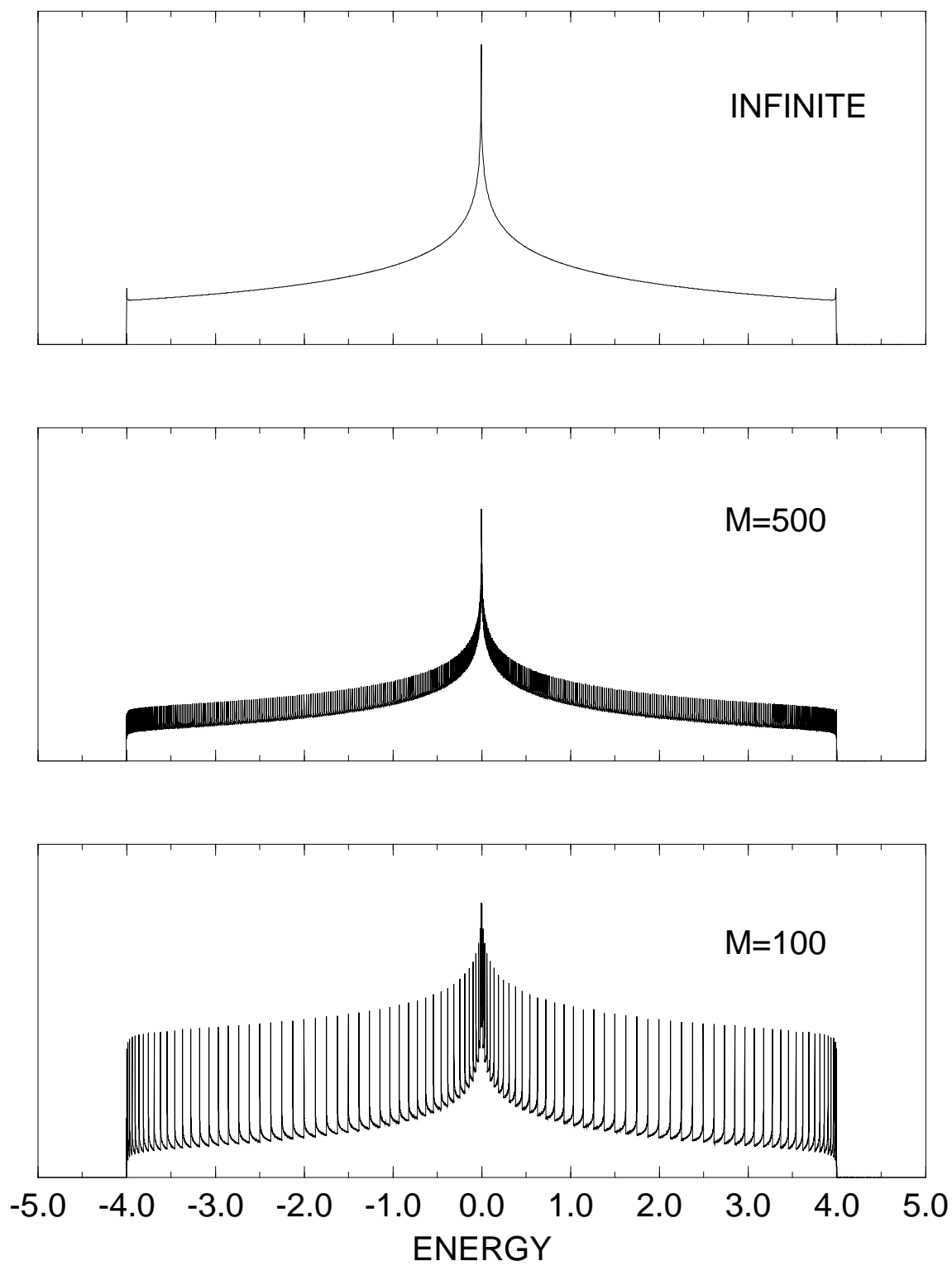
FIG. 6. DOS, in log scale, for the two dimensional case, for three nearby energy points, as a function of the short-range parameter σ .

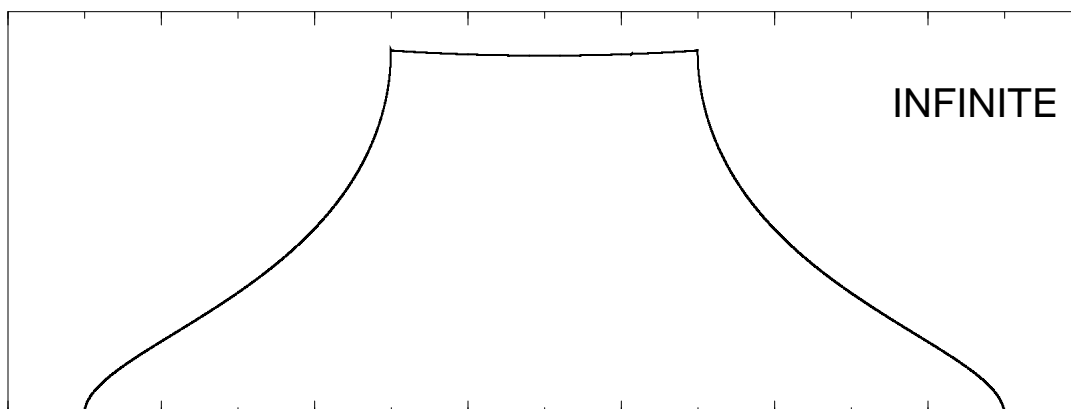
FIG. 7. Size effects for the random disordered binary alloy for the three dimensional case (case (b) of Fig.5). For finite systems we use the following correlation parameters: $p_{AB} = 1/4$, $z_3 = z_4 = 1/16$, and $\xi_1 = \xi_2 = 0$. Note that the lower DOS, for a bar of cross section of 12 atoms, already presents, except for the amplitude of some peaks, the main structure of the infinite system density.

FIG. 8. DOS, in arbitrary units, for a three-dimensional bar ($N \times M = 12$) for different values of the applied magnetic field. The case depicted corresponds to a disordered binary alloy near the segregation limit for equal concentrations of both species. Correlation parameters are $p_{AB} = 0.05$, $z_3 = z_4 = 0$, and $\xi_1 = \xi_2 = 0$. We only show the lower sub-band and the magnetic flux is indicated in each figure. Due to periodic boundary conditions for the finite section of the bar, the magnetic phase factor is quantized in units of $\pi/3$.

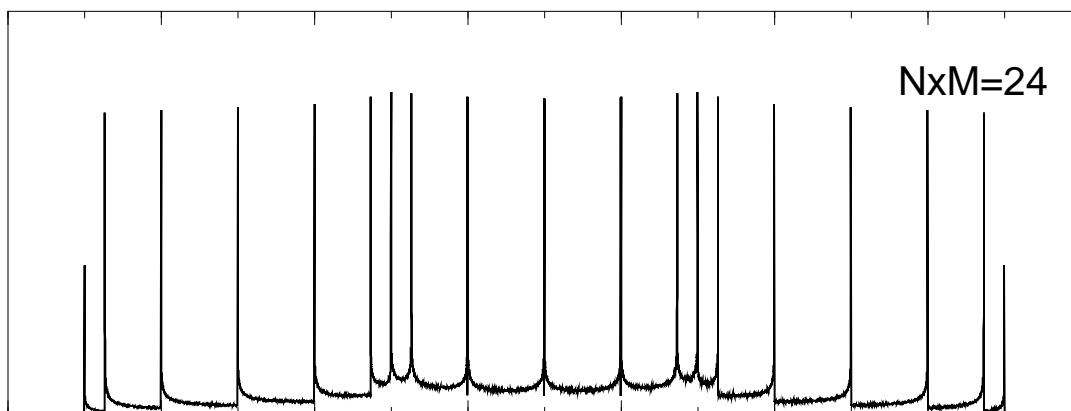
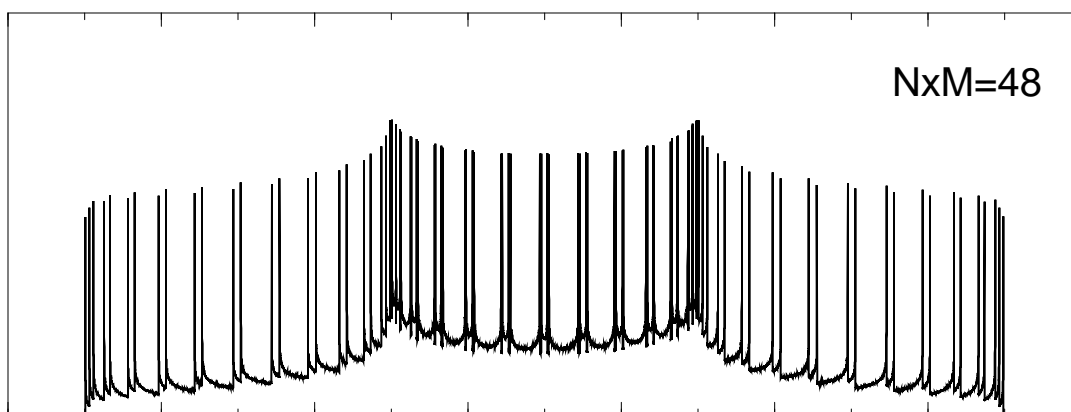
FIG. 9. DOS, in arbitrary units, at a particular energy point ($E = 3.0$), for a three-dimensional bar ($N \times M = 12$), for different values of the applied magnetic field, as a function of the short-range order.

DOS



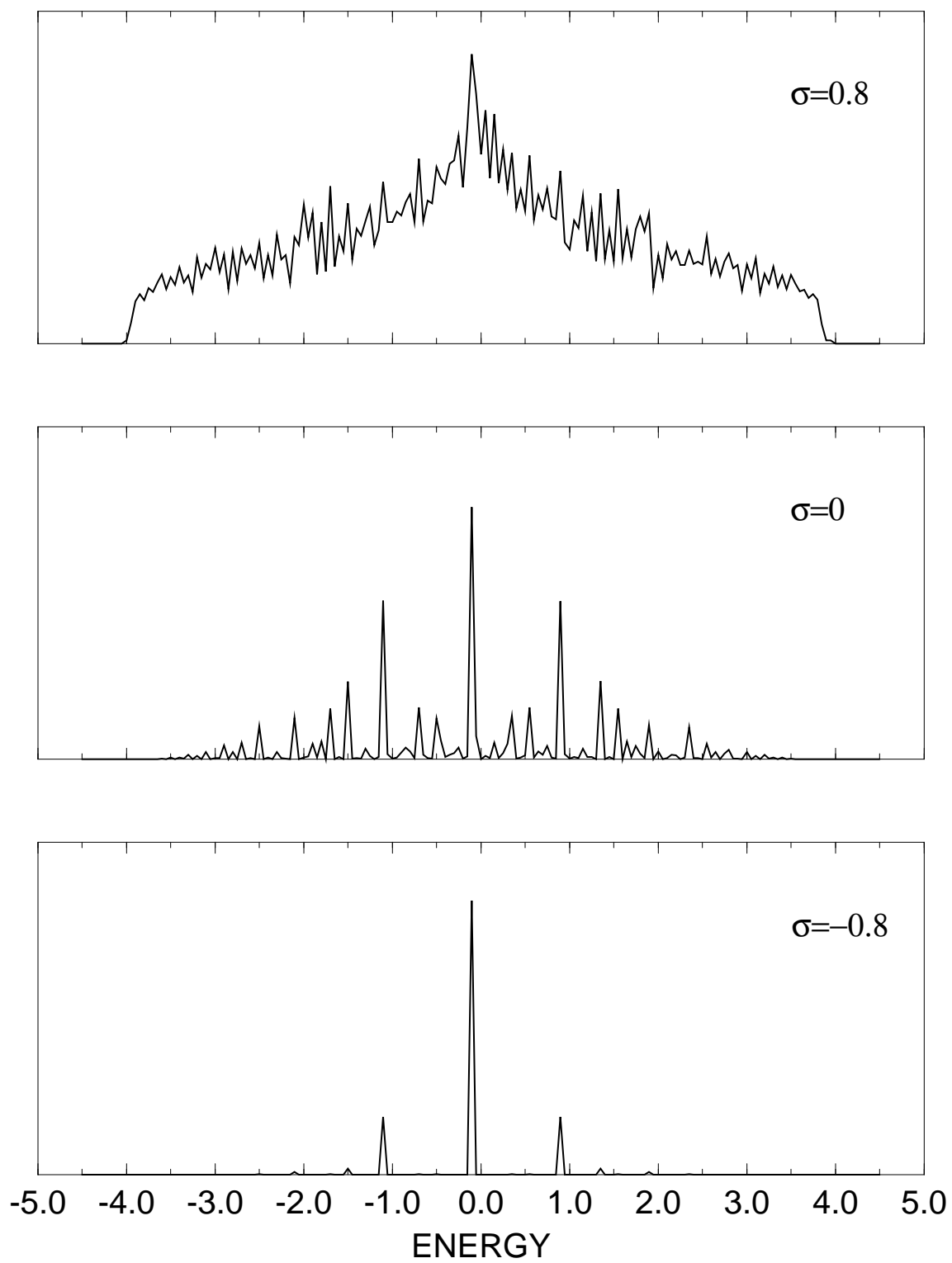


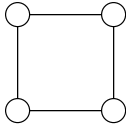
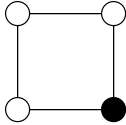
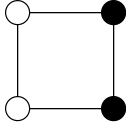
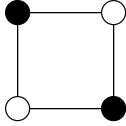
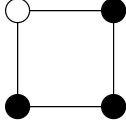
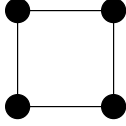
DOS

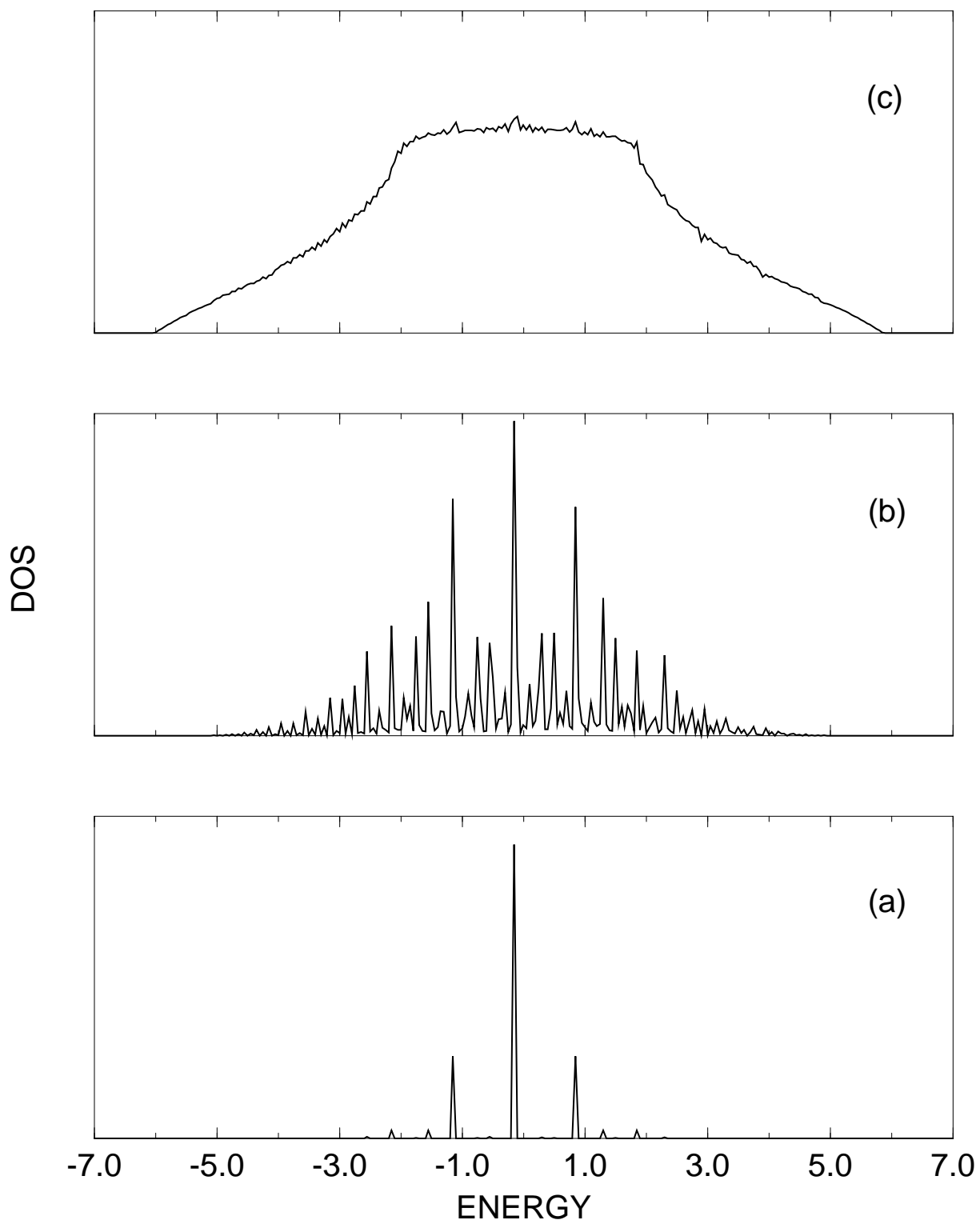


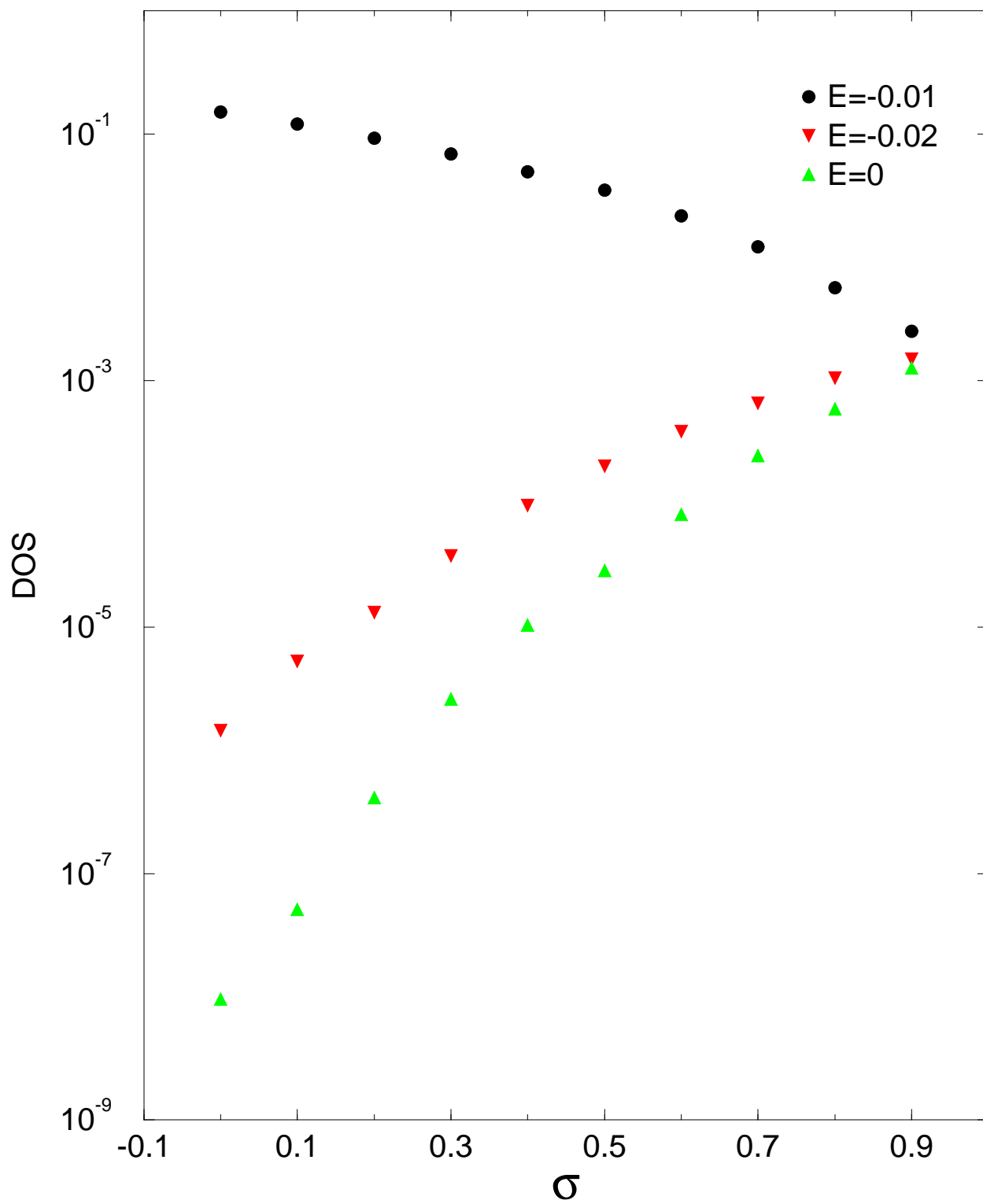
-7.0 -5.0 -3.0 -1.0 1.0 3.0 5.0 7.0
ENERGY

DOS



| SQUARE | PROB. | DEG. |
|-------------------------------------------------------------------------------------|-------|------|
|  | z_1 | 1 |
|  | z_2 | 4 |
|  | z_3 | 4 |
|  | z_4 | 2 |
|  | z_5 | 4 |
|  | z_6 | 1 |





DOS

